Bioprocess and Biosystems Engineering (2024) 47:1183–1196
https://doi.org/10.1007/s00449-024-02993-7

RESEARCH PAPER

Harnessing nature's potential: *Alpinia galanga* methanolic extract mediated green synthesis of silver nanoparticle, characterization and evaluation of anti-neoplastic activity

Ejaj Ahmad[1] · Alina Athar[1] · Nimisha[1] · Qamar Zia[2] · Abhay Kumar Sharma[1] · Mohammed Sajid[3] · Mausumi Bharadwaj[3] · Mairaj Ahmed Ansari[4] · Sundeep Singh Saluja[1,5]

Received: 27 October 2023 / Accepted: 6 March 2024 / Published online: 21 March 2024

Abstract

With the advent of nanotechnology, the treatment of cancer is changing from a conventional to a nanoparticle-based approach. Thus, developing nanoparticles to treat cancer is an area of immense importance. We prepared silver nanoparticles (AgNPs) from methanolic extract of *Alpinia galanga* rhizome and characterized them by UV–Vis spectrophotometry, Fourier transform Infrared (FTIR) spectroscopy, Zetasizer, and Transmission electron Microscopy (TEM). UV–Vis spectrophotometry absorption spectrum showed surface plasmon between 400 and 480 nm. FTIR spectrum analysis implies that various phytochemicals/secondary metabolites are involved in the reduction, caping, and stabilization of AgNPs. The Zetasier result suggests that the particles formed are small in size with a low polydispersity index (PDI), suggesting a narrow range of particle distribution. The TEM image suggests that the particles formed are mostly of spherical morphology with nearly 20–25 nm. Further, the selected area electron diffraction (SAED) image showed five electron diffraction rings, suggesting the polycrystalline nature of the particles. The nanoparticles showed high anticancer efficacy against cervical cancer (SiHa) cell lines. The nanostructures showed dose-dependent inhibition with 40% killing observed at 6.25 µg/mL dose. The study showed an eco-friendly and cost-effective approach to the synthesis of AgNPs and provided insight into the development of antioxidant and anticancer agents.

✉ Sundeep Singh Saluja
sundeepsaluja@yahoo.co.in

[1] Central Molecular Laboratory, Govind Ballabh Pant Institute of Postgraduate Medical Education and Research (GIPMER), New Delhi-110002, India

[2] Department of Medical Laboratory Sciences, Majmaah University, Majmaah, Saudi Arabia

[3] Division of Molecular Genetics & Biochemistry, Molecular Biology Group, ICMR-National Institute of Cancer Prevention & Research, Noida, Uttar Pradesh, India

[4] Center for Virology, SIST, Jamia Hamdard, New Delhi 110062, India

[5] Department of GI Surgery, Govind Ballabh Pant Institute of Postgraduate Medical Education and Research (GIPMER), New Delhi 110002, India

Graphical abstract
Schematic representation of synthesis and characterization of AgNPs.

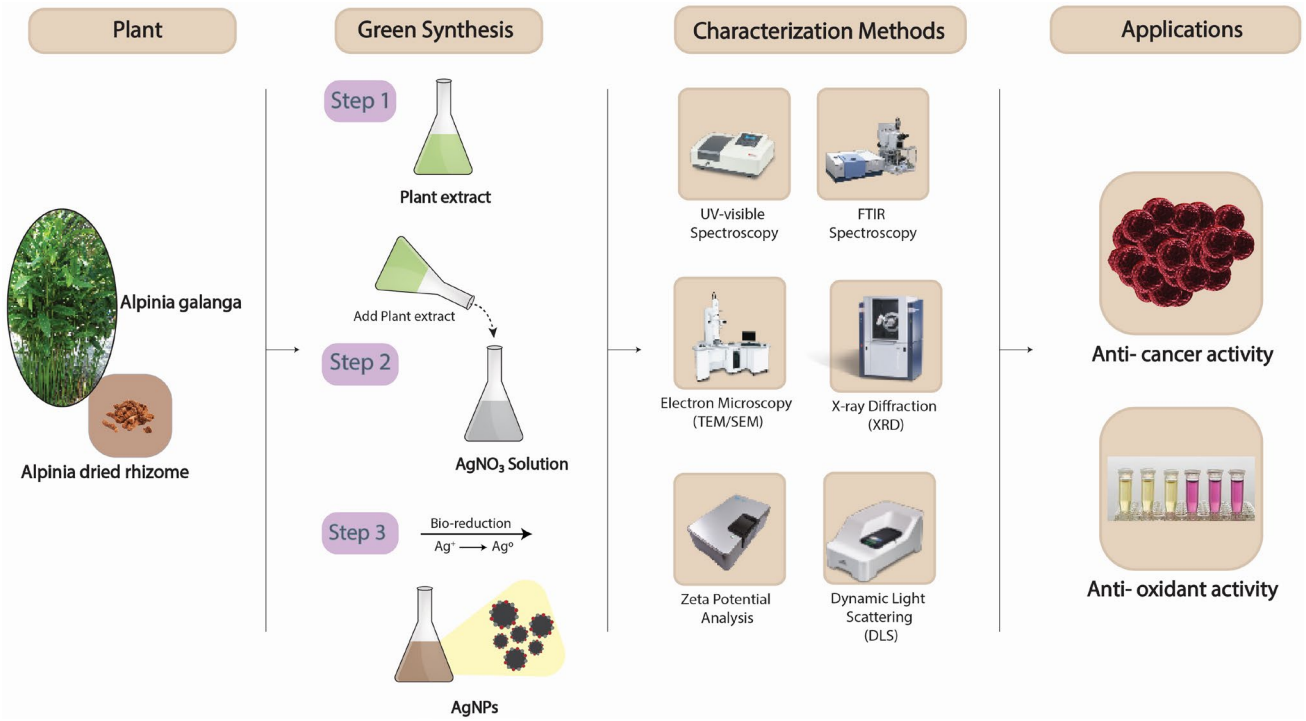

Keywords Silver nanoparticles · Green synthesis · Alpinia galanga · Antioxidant · Cancer

Introduction

In the biomedical field, nanotechnology offers unique opportunities for studying and managing a wide range of techniques at the nanoscale, with the potential to have a revolutionary impact on biology, medicine, and other health-related fields [1]. At the nanoscale level, alterations in size and shape occur due to the increased surface-to-volume ratio, which affects the physical properties of materials. Thus, these nanostructures can be engineered to enhance drug solubility, improve bioavailability, and enable targeted delivery, minimizing side effects and maximizing therapeutic efficacy [2]. In diagnostics, nanotechnology contributes to the development of highly sensitive imaging agents and biosensors, allowing for early disease detection and personalized medicine [3]. In addition, nanomaterials are employed in tissue engineering and regenerative medicine, fostering advancements in the repair and replacement of damaged tissues [4]. Various nanoparticles (NPs), such as solid lipid NPs, metallic NPs, polymeric NPs, carbon nanotubes, nanogel-based compounds, nanocapsules, nanofluids, nanowires, and liposomes are just a few examples of the diverse range of nanomaterials with biomedical prominence. Their potential use for therapeutic applications has been examined, with a focus on their appropriateness and biocompatibility, medication administration, and antimicrobial applications [5–9].

Among non-communicable diseases, cancer is the leading cause of death worldwide [10]. The conventional approaches for cancer management include surgery, chemotherapy, and radiotherapy. Recently, nanotechnology has been used in the diagnosis and therapeutic intervention of cancers, showing efficacy in cancer treatment [11]. Cancer nanotechnology opens new vistas in medical science wherein a multidisciplinary approach to explore chemistry, medicine, engineering, and biology has paved the way for remarkable advancements in cancer detection, diagnosis, and treatment [12]. The high surface area-to-volume ratio of nanoparticles provides an expansive canvas for functionalization and customization leading to significant improvement in reactivity [13]. Several nanoparticles encapsulating anticancer drugs have been developed to treat cancer. Many of them, such as Doxil® (Johnson & Johnson, New Brunswick, NJ, USA), Abraxane® (Celgene, Summit, NJ, USA), and Myocet™ (Perrigo, Dublin, Ireland), etc., received approval from the US Food and Drug Administration for clinical use [1]. These formulations have reduced the toxicity of anticancer drugs to some

extent in healthy cells [5]. Nonetheless, the production of organic nanoparticles tends to be relatively costly, and while these nanoparticles effectively mitigate a substantial portion of drug-induced toxicity, they still carry the potential for some degree of harm to healthy cells, which cannot be entirely eliminated [6].

The development of metal nanoparticles from noble metals such as silver, gold, platinum, etc., exhibits significant promise across diverse domains, including cancer [7–9]. However, the synthesis of metal nanoparticles by physical and chemical methods is associated with some disadvantages. Physical methods of synthesis demand substantial energy consumption and often result in solvent contamination, which raises environmental and safety concerns. Furthermore, achieving uniformity in nanoparticle size and properties through physical methods can be challenging, potentially compromising their effectiveness in various applications [14, 15]. The chemical modes of synthesis include chemical vapor synthesis, sol–gel, solvothermal and hydrothermal methods, plasma-assisted as well as reverse micelle techniques [16]. The mode of preparation involves the use of toxic and hazardous chemicals [17], restricting its usage in medical science. These drawbacks led to the development of an eco-friendly, less energy-consuming, and greener approach to nanoparticle synthesis, utilizing bio-origin molecules such as various parts of plants, algae, fungi, bacteria, etc. [18–20].

The green synthesis of AgNPs has garnered immense attention in recent years due to its one-step synthesis process, eco-friendly nature, cost-effectiveness, and high yield [21, 22]. Moreover, the ability to control size, shape, and composition with precision is often enhanced in biological methods. This innovative approach has demonstrated great potential across a wide array of applications [23]. Further, the presence of phytochemicals/secondary metabolites, polysaccharides, proteins, and many compounds with functional groups like amine, ketone, and aldehyde act, as reducing, capping, and stabilizing agents to synthesize AgNPs [24].

Green synthesized silver nanoparticles (AgNPs) have many biological uses, including anticoagulant [25], analgesic [26], anti-inflammatory [27], wound healing [28], antidiabetic [29], antivenom [30], and neurodegenerative [31]. Furthermore, the therapeutic potential of green-synthesized silver nanoparticles (AgNPs) has also been rigorously evaluated against a spectrum of targets, encompassing bacteria, fungi, and tumor cells [32], making them a compelling eco-friendly alternative to traditional antibiotics in medical settings [33]. Nowadays, advanced coating technologies are employed to integrate silver nanoparticles into various materials for antimicrobial purposes, such as coatings for wound dressings, medical devices, textiles, and surfaces in healthcare settings [28, 34]. This approach could potentially lead to the development of new therapeutic agents that could combat antibiotic-resistant microbial infections as well as neoplasms.

Alpinia galangal, commonly known as galangal or blue ginger, is a medicinal plant with a rich source of bioactive compounds, including antioxidants and polyphenols. These compounds serve as greener and more stable reducing agents for the one-pot synthesis of AgNPs [35]. The bioactive compounds present in *Alpinia galangal* contribute to the effective reduction of silver ions, leading to the synthesis of AgNPs with distinct properties [36] The ethanolic extract of *Alpinia galanga*-based AgNPs has shown significant efficacy in restricting the growth of bacteria [36].

To the best of our knowledge, this is the first report of biosynthesizing silver nano-assemblies using a methanolic extract of *Alpinia galanga rhizome*. The biogenic NPs were characterized by various techniques such as UV–Visible spectrophotometry, Fourier Transform Infrared spectroscopy (FTIR), Zetasier, and TEM. The antioxidant activity of the AgNPs was analyzed by DPPH method. The anticancer efficacy of AgNPs was evaluated on oral squamous carcinoma (CAL27) and cervical carcinoma (SiHa) cell lines.

Materials and methods

Material

Alpinia galangal (rhizome) procure from local market, Lucknow, India. Silver nitrate, Sulforhodamine- B (SRB), 2, 2-Diphenyl-1-picrylhydrazyl (DPPH), and KBr purchased from Sigma-Aldrich. Dulbecco's modified Eagle's medium/Nutrient Mixture F-12 (DMEM/F-12), Fetal bovine serum (FBS), Penicillin and Streptomycin, Gentamycin, 0.5% Trypsin–EDTA were purchased from Thermo Fisher Scientific (Waltham, MA). Milli-Q water was prepared in the Central molecular laboratory (GIPMER). Cancer cell lines, oral squamous cell carcinoma (CAL27), cervical carcinoma (SiHa), and noncancerous Human embryonic kidney cell line (Hek293) were obtained from ATCC.

Methods

Preparation of silver nitrate ($AgNO_3$) solution

Silver nitrate solution (10 mM) was made by dissolving 0.169 g of $AgNO_3$ in 100 mL of Milli-Q water, and the solution was filtered to remove any undissolved solid. To avoid photodegradation, the solution was prepared in an amber-colored reagent bottle.

Preparation of *Alpinia galangal* methanolic extract

The rhizomes obtained were washed thoroughly in running water and subsequently with Milli-Q water. The washed rhizomes were then dried in a hot air oven under a controlled temperature of 45–50 ℃ for two days. Fine powder of dried rhizome was prepared using mortar and pestle. Then, 50 mL of methanol was added into 5 g of dried powder in a volumetric bottle and kept overnight in a dark place at room temp. The (10% w/v) solution was sonicated using a bath type sonicator (Branson 5800) for 1 h and was filtered in a glass bottle using No.1 Whatman filter paper. The filtrate was stored at 4 ℃ for two weeks for further use [37].

Green synthesis of AgNPs

The biogenic synthesis of AgNPs is a hassle-free and environment-friendly technique that utilizes plant extracts, from different parts of the plant, for the reduction of silver ions into AgNPs. The formation of nanoparticles occurs mainly in three stages: ion reduction, cluster formation, and nanoparticle synthesis. The characteristics of each stage depend on several factors such as concentration of plant extract, molarity of $AgNO_3$, temperature, and pH of solution.

For the preparation of green synthesized nanoparticles, we used the methanolic extract of *Alpinia galangal*. To prepare small sizes, we tried different parameters, such as temperature, concentration of plant extract and $AgNO_3$, pH of the solution, rotation (rpm), and time duration. After varying each parameter, the particle size was analyzed using Zetasizer. However, we have obtained the smallest size of AgNPs with a 100:1 ratio of 1 mM $AgNO_3$ (30 mL) and 0.3 mL of *Alpinia galanga* rhizome methanolic extract. The solution was kept on a magnetic stirrer plate (Daihan Scientific, South Korea) at 500 rpm at 70 ℃ for 1 h. A gradual colour change from colourless solution to pale yellow and light brown to brown with the increase of time duration was observed. However, a prominent brown colour was observed after 1 h. This optical change in colour suggests that biomolecules reduced the silver ions into AgNPs.

The biosynthesised AgNPs were centrifuged at 12,000 rpm for 12 min (Eppendorf, Centrifuge 5425R; Hamburg, Germany). The supernatant was gently removed and the pellet containing AgNPs was washed 2–3 times with Milli-Q water. The washed AgNPs were dried in a vacuum oven at 45 ℃ for 2 h at 0.8 bar (Daihan Scientific, South Korea) and stored at −80 °C until biological activity was performed.

Characterization of AgNPs

UV–Vis spectrophotometry

UV–Visible spectrophotometer was used to analyze the *surface plasmon resonance (SPR)* of the synthesized silver nanoparticles. The intensity of electronic transitions between 300 and 600 nm was traced. To analyze the transition of electrons, the extract and AgNPs were scanned from 300 to 700 nm [38].

Functional groups analysis by FTIR analysis

The presence of functional groups of the phytochemicals responsible in the reduction and capping of the prepared nanoparticles from the methanolic extract of *Alpinia galanga* rhizome was analyzed using FTIR at a scanning range of 4000–400 cm^{-1} with spectral resolution 1 cm^{-1} in transmittance mode (Brucker, Optika GmbH, Karlsruhe, Germany) using KBr pellet method.

Zetasizer & zeta potential analysis

The mean particle size and their polydispersity index (PDI) were analyzed using a Malvern Zetasizer Pro Blue instrument (Malvern Analytical Ltd, Malvern UK) containing He–Ne laser (4 mW) at 633 nm under ambient temperature. For the measurement of zeta potential, the AgNPs were two to three folds diluted in Milli-Q water beforehand.

Transmission electron microscopy (TEM) analysis

TEM of the prepared AgNPs was further performed to analyze their morphology and corroborate its size with Zetasizer. The prepared AgNPs were sonicated for 5 min in a bath-type sonicator (Branson, 5800) beforehand. Then, AgNPs were 100 folds diluted in Milli-Q water, and 5 µL samples were put on a carbon-coated copper grid and air dried under a lamp. The TEM image of the AgNPs was examined with FEI Tecnai G220S-Twin acquired by operating at 200 kV. Micrographs were captured using a Gatan bottom mount camera using Digital Micrographs software.

X-ray diffraction analysis

X-ray diffraction (XRD) technique is used to analyze the phase and the crystalline structure of the synthesized AgNPs. The AgNPs were characterized by Rigaku D/Max-IIIC diffractometer with a monochromatic source of cu-kα and AXIS Supra using a monochromatic X-ray source of Al Ka-1486.6 eV between 2θ of 10 and 80°.

Antioxidant activity analysis

The antioxidant activity of the methanolic extract of *Alpinia galanga* rhizome and prepared AgNPs was analyzed by the procedure of DPPH radical scavenging assay [39] In brief, 100 µL of various concentrations of methanolic extract and AgNPs were taken in a 96-well ELISA plate, while the varying concentration of ascorbic acid in 100 µL was used as a standard. Subsequently, 100 µL of DPPH prepared in 80% ethanol (0.5 mM) was added into each well and allowed to react in dark for 0.5 h at room temperature. The absorbance of the reaction mixture and control was measured using a multimode reader at 517 nm (Thermo-scientific). The formula given below is used to calculate the percentage of free radical scavenging activity.

$$\text{DPPH radical scavenging assay (\%)} = \frac{(\text{Abs of control} - \text{Abs of sample})}{\text{Abs of control}} \times 100$$

Culturing of cell lines

The cervical cancer cell line (SiHa), oral squamous cell carcinoma cell line (CAL27), and noncancerous human embryonic kidney (Hek293) cell lines were cultured in DMEM/F-12 media with the addition of 10% FBS, 1% Penicillin–Streptomycin and Gentamycin (50 mg/L) at 37 °C in a CO_2 incubator with 5% CO_2.

Analysis of anti-proliferative activity on cancer cell lines

To quantify the cytotoxic activity of AgNPs prepared from methanolic extract of *Alpinia galanga*, the sulforhodamine-B (SRB) colorimetric assay was performed by following a published procedure [40] SiHa and CAL27 cancer cells, and noncancerous Hek293 cells were seeded in a 96-well plate (10^4 cells/well) and incubated for 24 h at 37 °C in the CO_2 incubator. The DMEM medium was removed and different concentrations of AgNPs (3.125, 6.25, 12.5, 25, 50, and 100 µg/mL) dissolved into the medium were added to their respective wells (triplicates). After 24 and 48 h incubation, cells were washed once with PBS and fixed in trichloroacetic acid (10% w/v) for 1 h at 4 °C. Subsequently, the plate was washed (quadruple times) with sterile Milli-Q water, and cells were stained by adding100 µL of 0.057% SRB solution (Sigma-Aldrich, Bangalore, India) for 0.5 h at ambient temperature. Once the incubation was over, cells were quickly rinsed with 1% acetic acid solution (quadruple times), and the plate was kept for drying at ambient temperature. Protein-linked SRB was dissolved (200 µL/well) using 10 mM tris-base solution (pH 10.5) under shaking conditions (5 min at 200 rpm) and absorbance was taken at 564 nm using a SPECTROstar Nano plate reader (BMG Labtech, Ortenberg, Germany).

Statistical analysis

The data obtained were analyzed in a grouped two-way ANOVA following Dennett's *t* test method. *P* value <0.05 was considered significant between the treated and control groups.

Result and discussion

The biogenic synthesis of AgNPs is a hassle-free and environmentally friendly technique that utilizes plant extracts, from different parts of the plant, to reduce silver ions into AgNPs. The formation of nanoparticles occurs mainly in three stages: ion reduction, cluster formation, and nanoparticle synthesis. The characteristics of each stage depend on several factors such as concentration of plant extract, molarity of $AgNO_3$, temperature, and pH of solution. Plant biomolecules that contain hydroxyl groups, such as amino acids, proteins, alkaloids, flavonoids, polyphenols, enzymes, tannins, carbohydrates, and saponins, are responsible for the reduction, capping, and stabilization of silver ions. The formation of silver nuclei leads to the production of AgNPs. Unlike conventional chemical synthesis methods, this approach does not require the use of harsh chemicals or high temperatures, making it a safer and more sustainable option.

UV–Vis spectral analysis

The appearance of light yellowish-brown colour in aqueous medium was due to surface plasmon vibration [41] As the varying quantities of methanolic Alpinia rhizome extract were added to the fixed molar clear silver nitrate solution (1 mM), the colour of the solution gradually changed from light yellow and then light brown, which suggests the formation of AgNPs have formed. Numerous studies have implied that the formation of AgNPs led to the change of colour [42, 43], confirming the completion of the reaction between methanolic *Alpinia galanga* extract and $AgNO_3$. The UV–Vis spectrum was recorded after the formation of a light brown colour (Fig. 1). The absorption spectrum of the formed AgNPs suggests that the absorption increases again at 400 nm and reaches at maxima peak at around

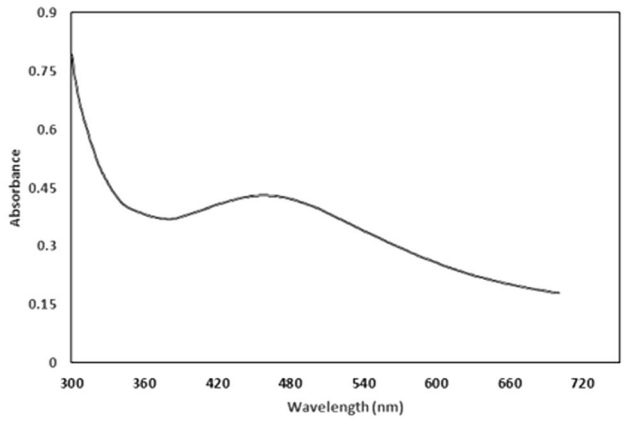

Fig. 1 UV–Vis spectrum of the methanolic extract of *Alpinia galangal* rhizome based AgNPs

454–462 nm, which was due to the *SPR* of electrons present on the surface of AgNPs [44]. A relationship between the absorption peak and crystal structure of the AgNPs has been established [45]. The authors have suggested that absorption peaks at 385, 435, and 515 nm correspond to the cubical structure of AgNPs, while those showed absorption maxima at 400, 430, and 462 nm are suggestive of spherical, cuboctahedral, truncated cubes, or crystalline structure of formed nanoparticles, respectively [45]. The maximum absorption peak at 454–462 nm, suggests the crystallinity of the particle is face centered cubic (fcc) in nature.

FTIR analysis of AgNPs

FTIR spectroscopy is often used to detect the secondary metabolites/phytochemicals or other compounds containing aldehyde, alcohol, and ketone as a functional group, which are responsible in the reduction of silver ions into AgNPs. The FTIR spectrum of *Alpinia*

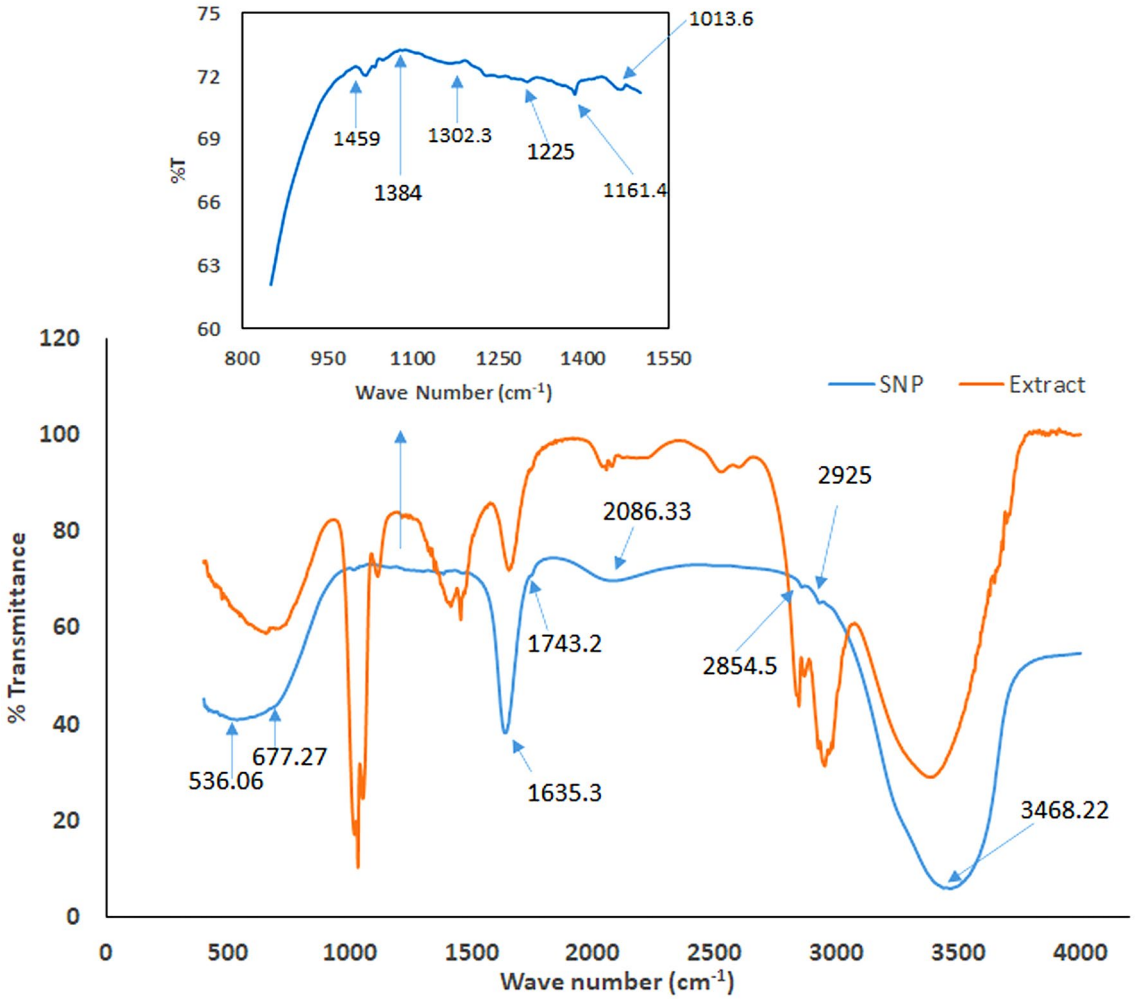

Fig. 2 FTIR spectrum of AgNPs prepared from the methanolic rhizome extract of *Alpinia galanga*

galanga methanolic extract exhibits major absorption peaks at 3391.5, 2949.6, 2865.4, 2053, 1652, 1454, 1346, 1216, 1114, 1018, and 655.5 cm^{-1} Similarly, little shift in the FTIR spectrum of the prepared AgNPs showed major peaks at 3468.2, 2925, 2854.5, 2086.3, 1634.3, 1459, 1384, 1302.3, 1225, 1161.4, 1013.6, 677.27, and 536.06 cm^{-1}. The appearance of AgNPs peaks suggests that the presence of phytoconstituents acts as a reducing, capping, and stabilizing agents (Fig. 2). Thus, from these peaks shift, we can speculate the probable functional groups containing compounds in the extract involved in the conversion of silver ions into AgNPs. A shift in the peak at 3391.5–3468.2 cm^{-1} is due to the involvement of the O−H or N−H stretching of phenolic compounds present in the extract [46]. The absorption bands at 2925 cm^{-1} suggest the presence C–H stretching of the aliphatic functional group/ methylene group and is also the characteristic peak of triterpenoid saponins [47]; peaks at 2854 cm^{-1} showed asymmetric and symmetric stretches of alkenes. The shift of slightly higher wavelength from 2053 to 2086.3 cm^{-1} suggests the presence of alkyne groups in the phytochemical constituents [48]. The absorption peak at 1635.86 cm^{-1} corresponds to the C=C group in the aromatic compounds [49]. The absorption band detected at 1459 cm^{-1} indicate S=O (sulphate ester) group. The peak at 1384 cm^{-1} spectrum suggests the presence of germinal methyl groups; the peak observed at 1225 cm^{-1} is due stretching vibration of C–C phenol and tertiary alcohol. The peaks at 1161.4 and 1013.6 cm^{-1} suggest the stretching of C–O of the ether group [43], while the absorption band at 677.27 cm^{-1} is due to the =CH group of the aromatic compounds. The peak at 536.06 cm^{-1} showed the presence of C=C of alkyne [50]. Thus, the FTIR analysis confirmed that various phenolic compounds present in the methanolic extract of *Alpinia galanga* rhizome are responsible for the reduction of silver ions and, subsequently, capping and stabilization leading to the synthesis of AgNPs.

Size and zeta potential analysis of silver nanoparticle

DLS technique was used to analyze the particle hydrodynamics size distribution, PDI, and surface charge (ζ-potential) of the green synthesized AgNPs. Nanoparticles were two to three folds diluted in Milli-Q water during size measurement to minimize the background of scattering. The mean particle size was observed to be 102 nm with a PDI of 0.24 (Fig. 3a). Further, the size and the respective percentage of different sizes of particles are shown on the secondary axis of Fig. 3c, which would enable the reader to comprehend the particle size

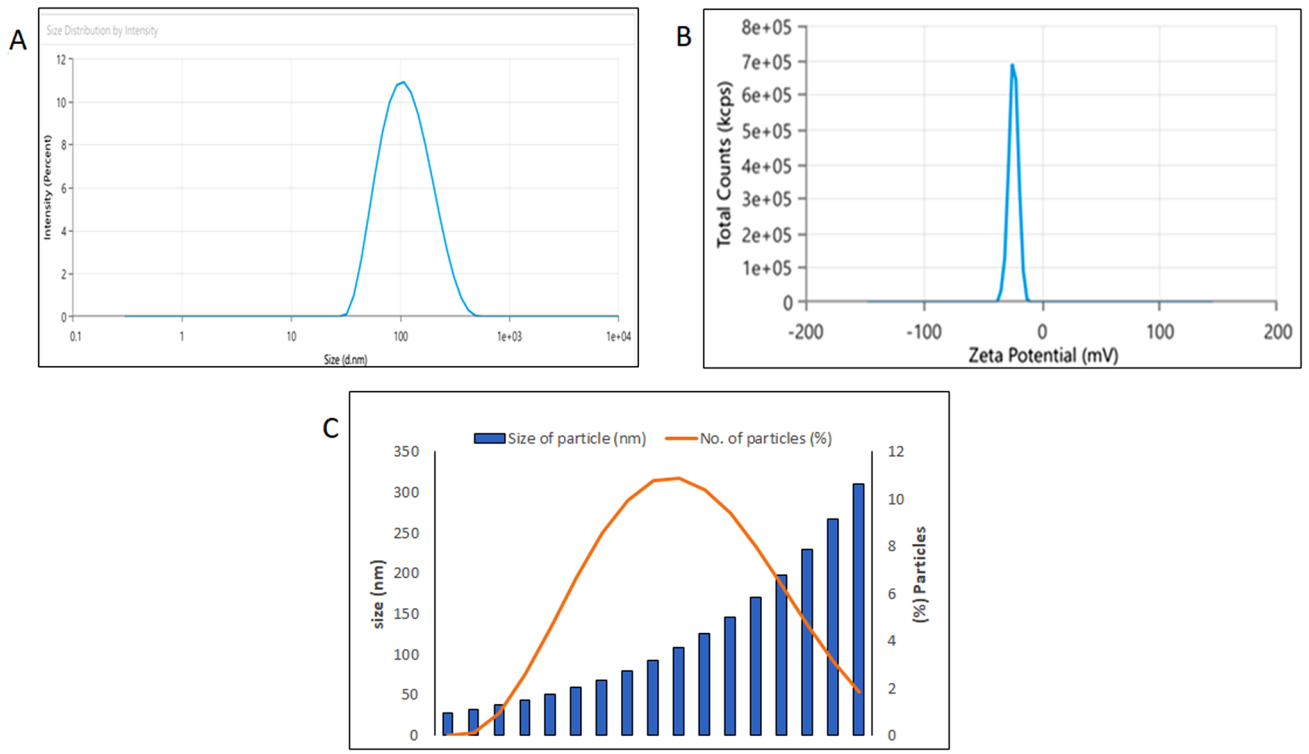

Fig. 3 Nanoparticle size measurements **a** Mean size **b** Zeta potential **c** size vs. (%) nanoparticles

distribution. The principle of DLS techniques is to measure the hydrodynamic size that includes the hydration layer present around the AgNPs; thus, the hydrodynamic size of the particles is usually larger compared to TEM images. Furthermore, the adsorption of phytochemical constituents of the methanolic extract of *Alpinia galanga* rhizome might contribute to the hydrodynamic size. Variation in the particle size might be due to the presence of different proportions of the phytoconstituents on the particles. AgNPs of this range have been synthesized from different parts of the plants [51]. The measurement of the ζ-potential of the particles is important because it suggests particle stability. The high negative and positive ζ-potential suggests higher stability, which correlates the better colloidal properties owing to electrostatic repulsion and higher dispersity [52]. The observed ζ-potential of the synthesized nanoparticle is -23mV advocating stability of the AgNPs (Fig. 3b). Further, the presence of negatively charged functional groups on the surface of nanoparticles shows the colloidal stability of the synthesized AgNPs [53].

Transmission electron microscope analysis

The TEM images were acquired at different magnifications to analyze the morphology of the formed AgNPs (Fig. 4a–c). The images clearly suggest that most of the formed particles are spherical with nearly 20–25 nm in size; however, some of the particles of cylindrical shape are also evident. The size of the particles is corroborating the Zetasizer result. At very high magnification (650,000X), the fringes of the particles are also visible, suggesting uniform distribution of phytochemical constituents on silver ions (Fig. 4d).

Selected area electron diffraction (SAED) analysis of AgNPs

The SAED image provides information related to the crystalline structure of the AgNPs [54]. The result of the SAED image showed bright five electron diffraction rings, which can be seen in Fig. 4f. The presence of a bright ring suggests the polycrystalline nature of the formed AgNPs [54]. Earlier, Kanniah et al., have observed five electron diffraction ring patterns in the AgNPs, which correspond to the lattice

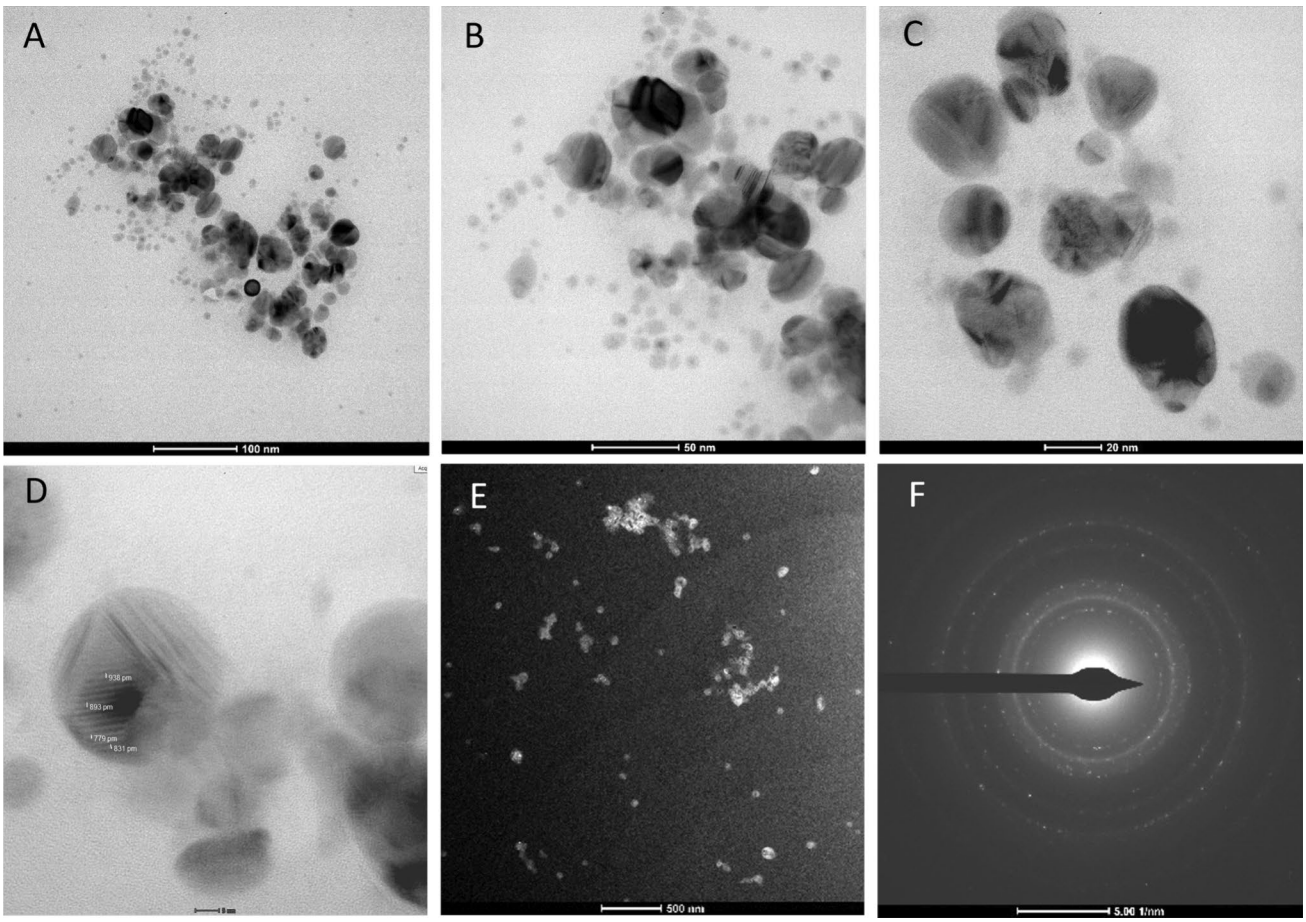

Fig. 4 **a**–**c** TEM image of AgNPs with different magnifications **d** HR-TEM image with fringes **e** Dark Field image **f** SAED image of AgNPs

pattern of [111], [200], [220], [311], and [222], suggesting the fcc structure of the AgNPs [55]. Thus, the presence of five electron diffraction rings of the lattice planes might correspond to Bragg's lattice pattern confirming the fcc structure of the synthesized AgNPs. Our obtained data on crystal planes are in concordance with the earlier findings [56–58].

X-ray diffraction (XRD) analysis

The XRD analysis was performed to understand the nature of the synthesized AgNPs. The crystallinity of the synthesized AgNPs is an important parameter that needs to be proven pragmatically. Thus, besides SAED image analysis, XRD was performed to verify the SAED result, and also provide the supportive evidence of the crystallinity of the synthesized AgNPs. The analyzed XRD pattern, however showed four 2θ diffraction prominent peaks that include 32.304, 46.17, 54.76, and 77.330° (Fig. 5). These peaks in the spectrum correspond to the [111], [120], [202], and [311] planes, respectively, suggesting the fcc and the crystalline nature of the synthesized AgNPs, which is in concordance with the SAED image of the synthesized AgNPs. Elumalai et al. observed XRD peaks of the green synthesized AgNPs from the extract of *Leucas aspera*, which corresponded to [110] [111], [121], [200], and [311] planes, suggesting the polycrystalline fcc structure [59]. Dehghanizade et al., observed an additional XRD peak at 81.7° corresponding to the plane [222] of the synthesized AgNPs from *Anthemis atropatana* extract, suggesting the fcc structure of the particles [43]. Thus, these peaks suggest that the crystallization of the metabolite present on the surface of silver ion (Ag^+) promotes the formation of AgNPs, which is in accordance with earlier findings [60]. The result provides pragmatic evidence that the presence of phytochemicals in the *Alpinia galanga* methanolic extract causes reduction of silver ions and the synthesis of polycrystalline AgNPs.

Antioxidant activity analysis using DPPH Assay

The antioxidant activity of the methanolic extract and AgNPs was analyzed by a DPPH assay. The result suggests that both extracts and AgNPs showed a dose-dependent increase in the scavenging effect at lower concentrations (Fig. 6). Ascorbic acid was used as a standard. Further, the AgNPs result showed a significantly higher free radical inhibition compared to the extract; the IC_{50} values of the free radical inhibition of AgNPs and extract are 7.56 and 38.92 µg/mL, respectively.

Anticancer activity

To minimize the loss of precious human lives due to cancer, innovative approaches are required for better management. The traditional treatment approaches have their limitations. In contemporary times, nanotechnology has exploited the utility of different materials to synthesize nanoparticles, and their usefulness was evaluated in the treatment of cancers [5, 6]. Of these approaches, inorganic nanoparticles have shown great potential to scientists due to their attributes, which could prove useful in the treatment of cancer, provided the dosage, frequency, and toxicity are carefully analyzed [61]. Moreover, numerous studies have been conducted to evaluate the anticancer activity of AgNPs in different cancer cell lines [44, 62].

The efficacy of the prepared nanoparticles was analyzed on two cancer cell lines, viz. oral squamous cell carcinoma (CAL27) and cervical cancer cell lines (SiHa) at

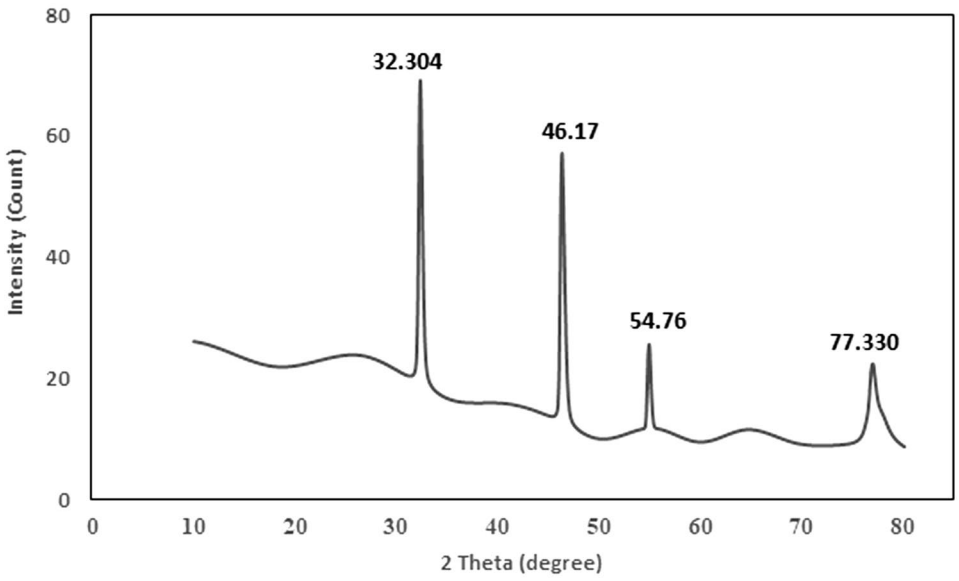

Fig. 5 X-ray Diffraction spectrum of AgNPs prepared from methanolic extract of *Alpinia galanga rhizome*

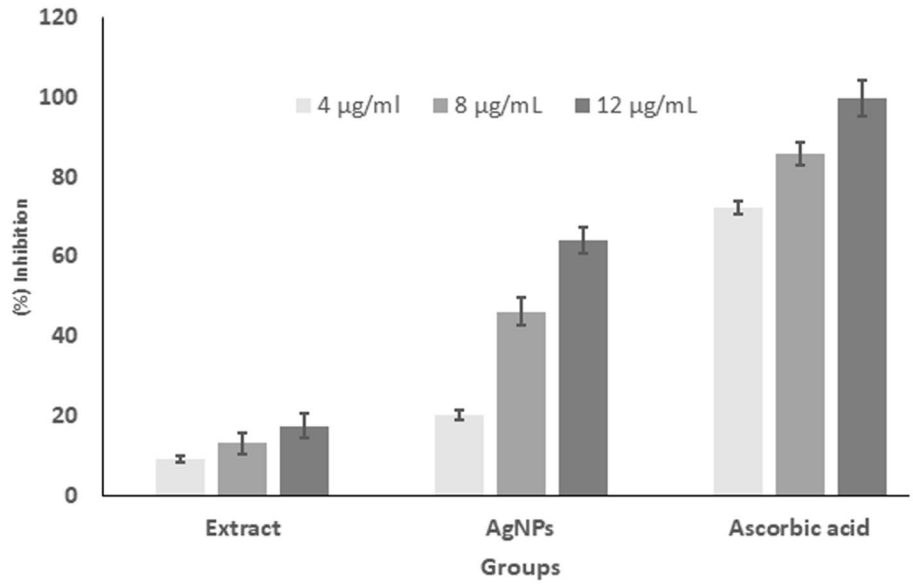

Fig. 6 Antioxidant activity of the methanolic extract of *Alpinia galanga* rhizome AgNPs and ascorbic acid. *P values* among the statistically significant in the AgNPs group of different doses 4 vs. 8 µg/mL; 4 vs. 12 µg/mL, <0.001)

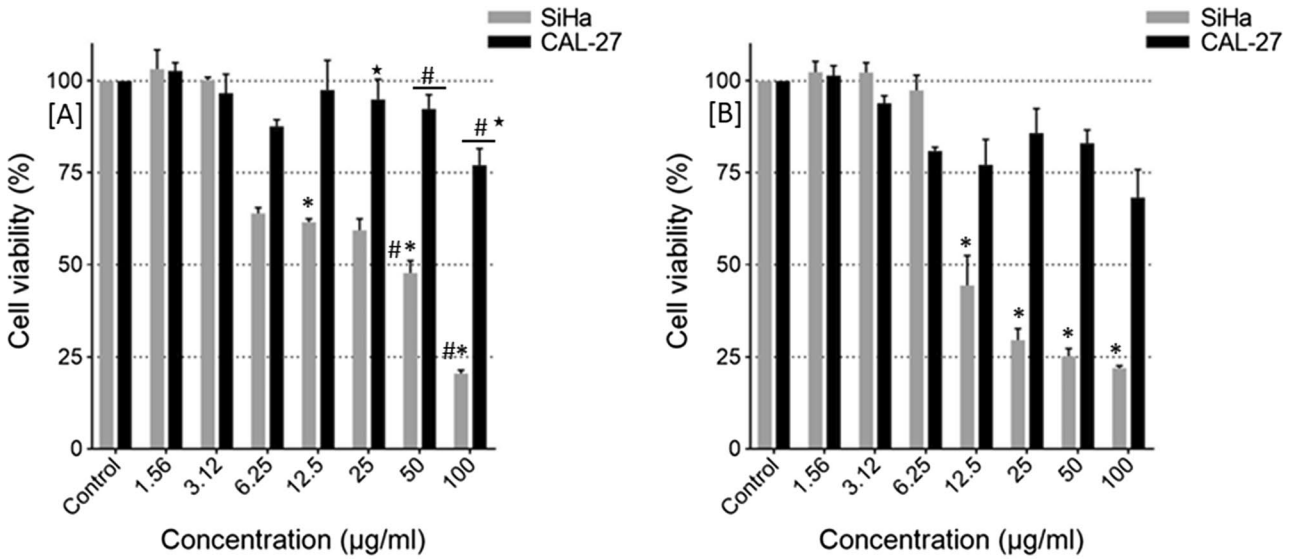

Fig. 7 Cytotoxicity of AgNPs after 24 h (**a**) and 48 h (**b**) to SiHa and CAL27 cancer cells exposure (SRB assay) The percentage of viable cells is expressed on the y-axis. The control (untreated) viable cells are assumed to be 100% viable. The concentration (µg/ml) of AgNPs are plotted on the x-axis. All data were expressed as means ± SEM (standard error of the mean) for $n = 3$ independent experiments. *P values* among the statistically significant to the SiHa cells post 24 h treatment (12.5 vs. 50 µg/mL; and 12.5 vs. 100 µg/mL; 50 vs. 100 µg/mL, <0.05) and 48 h post treatment (12.5 vs. 25 µg/mL; 12.5 vs. 50 µg/mL; 12.5 µg/mL vs. 100 µg/mL, <0.05). *P* values among the statistically significant to the CAL27 cell lines post 24 h treatment (25 vs. 100 µg/mL; 50 vs. 100 µg/mL, <0.05)

varying concentrations, such as 3.125, 6.25, 12.5, 25, 50, and 100 µg/mL using sulforhodamine-B (SRB) assay. The result suggests that very limited anticancer activity of the particles was observed on oral squamous cell carcinoma cell lines, i.e., at 100 µg/mL, 25 and 30% cells are killed at 24 and 48 h of incubation, respectively (Fig. 7). However, the formulation showed dose-dependent activity of AgNPs on SiHa cell lines. At a low concentration (6.25 µg/mL), nearly 40% of SiHa cells are killed; however, with further increase of doses up to 25 µg/mL, no significant increase of cancer cell killing was observed. Further increase of AgNP concentration to 50 µg/mL, nearly 55% of cancer cells were killed, while at 100 µg/mL, around 80% of cells were killed at 24 h of incubation, which was superior to the earlier prepared AgNPs [63–65]. The result suggests that the prepared AgNPs are highly effective against SiHa cell lines.

Fascinated by the result, the AgNP incubation duration was increased to 48 h to evaluate their efficacy. At 12.5 µg/mL dose, nearly 60% of cells were killed. Further increase of the formulation concentration, a dose-dependent killing of SiHa cells was observed. At 25, 50, and 100 µg/mL of AgNP concentrations, nearly 75, 80, and 84% of SiHa cells were killed, respectively. However, with the increase of time duration of AgNPs incubation, no significant number of SiHa cells killed was observed at 100 µg/mL (Fig. 7). From the results, we conclude that the prepared nanoparticles are highly effective against SiHa cell lines.

To date, the exact mechanisms underlying the anticancer activity of AgNPs are not fully elucidated. Dey et al., have suggested that AgNPs induce the production of reactive oxygen species (ROS), which damages the mitochondrial membrane, leading to the death of cancer cells [66]. AgNPs have been implicated in oxidative-stress-mediated inflammatory responses [67], and can induce ROS production, resulting in the phosphorylation of ERK and JNK, but not p38 [68]. This suggests a potential involvement of downstream proteins from ERK in modulating cell cycle progression and apoptosis [69]. In another study, AgNPs have been shown to activate p38 MAPK and are associated with DNA damage, leading to the inhibition of cell cycle progression and apoptosis, indicating mechanisms for both cytotoxicity and genotoxicity in Jurkat T cells [70]. In addition, AgNPs, when present within the nucleus, have been shown to induce oxidative base damages, strand breaks, and mutations in DNA, collectively contributing to genotoxic effects, as evidenced by the presence of 8-Oxoguanine (8-oxoG) [71]. However, it is important to highlight that while these mechanisms are proposed, the specific effects of AgNPs can vary depending on factors such as size, shape, concentration, colloidal state, and surface coating. Furthermore, the potential toxicity of silver nanoparticles to normal cells and tissues remains a concern [72], emphasizing the need for further research to understand their safety profile before considering them for clinical applications in cancer therapy.

Cytotoxicity analysis

Encouraged by the efficacy of the prepared AgNPs especially against the SiHa cancer cell line, it was necessary to evaluate the efficacy of the formulation against the noncancerous cell line. The HEK293 cell line is a well-characterized model cell line, which is widely used to evaluate the cytotoxic effects of chemicals and AgNPs [73, 74]. This cell line was chosen due to it delicate structure in the kidney filtration system, playing a pivotal role in the filtration of bodily fluids and the excretion of waste products. It is quite possible that inappropriate exposure to the AgNPs may affect renal cell structure and function. Thus, to investigate this possibility, we have evaluated the efficacy of the prepared AgNPs with varying doses

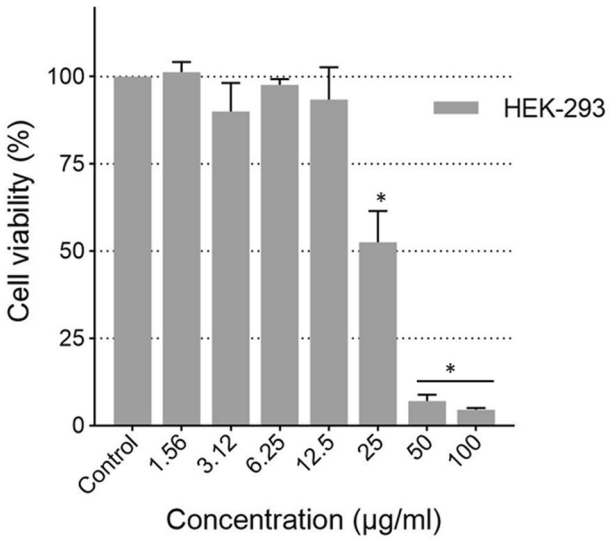

Fig. 8 Cytotoxic effect of AgNPs on the noncancerous Hek293 cells. *P values* are statistically significant among different doses (25 vs. 50 µg/mL; 25 vs. 100 µg/mL, <0.05)

to analyse the cytotoxicity. At the dose up to 12.5 µg/mL, no significant untoward effect of the prepared AgNPs was evident on the HEK293 cells. However, with the increase of AgNPs doses, the toxicity of the AgNPs was evident in a dose-dependent manner (Fig. 8). At 25 µg/mL concentration, 40–45% HEK293 cells showed growth inhibition. Further increase in doses resulted in more prominent inhibition of HEK293 cells. Thus, we conclude that the prepared AgNPs showed some level of toxicity to the noncancerous HEK293 cells. Therefore, it is advised to check the toxicity of the synthesized AgNPs on the other noncancerous cell lines before introducing them in clinical settings.

Conclusion

The green synthesis of AgNPs has drawn the attention of the scientific community around the globe. The process of synthesis is simple, energy-efficient, eco-friendly, and cost-effective. Further, its production can be easily scaled up. The green synthesis of AgNPs has shown efficacy against microbes and anticancer cells. Thus, it can be used as a potential candidate to improve human lives and could be proven effective in treating various diseases including cancers. We have synthesized AgNPs from methanolic extract of *Alpinia galanga* rhizome and characterized them with various techniques that include UV–Vis spectrophotometry, FTIR, Zetasizer, and TEM. The FTIR analysis suggests that various phytochemical/secondary metabolites are involved in the reduction, capping, and stabilization of silver ions into AgNPs. Zetasizer results showed that particles with a

mean size of 102 nm and PDI of 0.24. The size was corroborated by TEM images. High-resolution transmission electron micrography (HR-TEM) images showed fringes on the surface of nanoparticles, suggesting a uniform distribution of phytochemicals in the synthesis of AgNPs. The polycrystallinity of the prepared nanoparticles was established by five electron diffraction rings of the SAED image and XRD analysis. The anticancer activity of the prepared AgNPs showed remarkable activity against SiHa cell lines, while its activity against CAL27 cell lines showed limited activity. Moreover, the IC_{50} of the AgNPs against SiHa cell lines was 51.56 µg/mL, which is lower than AgNPs prepared from different plants and their IC_{50} was evaluated against different cancer cell lines [75–77]. We conclude that the prepared AgNPs are highly effective against SiHa cell lines. The study showed eco-friendly and less expensive method for the synthesis of antioxidant and anticancer agents.

Supplementary Information The online version contains supplementary material available at https://doi.org/10.1007/s00449-024-02993-7.

Acknowledgements The authors acknowledge the facilities provided by Govind Ballabh Pant Institute of Postgraduate Medical Education and Research (GIPMER), New Delhi, India. We thank to Professor Vineeta Batra, Department of Pathology, GIPMER, New Delhi for helping us to take TEM images of the nanoparticles. We are also thankful to the Advanced Instrumentation Research Facility (AIRF) Jawaharlal Nehru University, New Delhi to acquire FTIR spectrum of AgNPs and rhizome extract of *Alpinia galanga*. Authors are grateful to the Department of Biotechnology (DBT) for providing financial support under the head of "Establishment of Central Molecular Lab in GIPMER to study the diagnosis for precision medicine in order to understand the disease process and utilize it as Clinical Research Facility" with grant no. BT/INF/22/SP33063/2019.

Author contribution Conception EA, SSS; Data curation AA, EA, and MS; Formal Analysis EA, QZ, SSS, MB, MAA; Original draft AA, EA and MS; Revise the draft critically EA, Nimisha, AKS, QZ, MAA, MB and SSS; Approved SSS.

Funding The Department of Biotechnology (DBT), Government of India, has provided financial support under the head of "Establishment of Central Molecular Lab in GIPMER to study the diagnosis for precision medicine to understand the disease process and utilize it as a Clinical Research Facility" with grant no. **BT/INF/22/ SP33063/2019.**

Data availability The data and materials of the paper can only be accessed once the paper is available online.

Declarations

Conflict of interest The authors have no conflict of interest.

Ethical approval Not applicable.

References

1. Foulkes R, Man E, Thind J et al (2020) The regulation of nanomaterials and nanomedicines for clinical application: current and future perspectives. Biomater Sci 8(17):4653–4664. https://doi.org/10.1039/D0BM00558D
2. Ezike TC, Okpala US, Onoja UL (2023) Advances in drug delivery systems, challenges, and future directions. Heliyon 9(6):e17488. https://doi.org/10.1016/j.heliyon.2023.e17488
3. Alrushaid N, Khan FA, Al-Suhaimi EA et al (2023) Nanotechnology in cancer diagnosis and treatment. Pharma 15:1025. https://doi.org/10.3390/pharmaceutics15031025
4. Han F, Meng Q, Xie E et al (2023) Engineered biomimetic micro/nanomaterials for tissue regeneration. Front Bioeng Biotechnol 11:1205792. https://doi.org/10.3389/fbioe.2023.1205792
5. Yao Y, Zhou Y, Liu L et al (2020) Nanoparticle-based drug delivery in cancer therapy and its role in overcoming drug resistance. Front Mol Biosci 7:193. https://doi.org/10.3389/fmolb.2020.00193
6. Tenchov R, Bird R, Curtze AE et al (2021) Lipid nanoparticles─from liposomes to mRNA vaccine delivery, a landscape of research diversity and advancement. ACS Nano 15(11):16982–17015. https://doi.org/10.1021/acsnano.1c04996
7. Shariatzadeh S, Moghimi N, Khalafi F et al (2022) Metallic nanoparticles for the modulation of tumor microenvironment; a new horizon. Front Bioeng Biotechnol 10:847433. https://doi.org/10.3389/fbioe.2022.847433
8. Khursheed R, Dua K, Vishwas S et al (2022) Biomedical applications of metallic nanoparticles in cancer: current status and future perspectives. Biomed Pharmacother 150:112951. https://doi.org/10.1016/j.biopha.2022.112951
9. Xu JJ, Zhang WC, Guo YW et al (2022) Metal nanoparticles as a promising technology in targeted cancer treatment. Drug deliv 29(1):664–678. https://doi.org/10.1080/10717544.2022.2039804
10. Sung H, Ferlay J, Siegel RL et al (2021) Global cancer statistics 2020: GLOBOCAN estimates of incidence and mortality worldwide for 36 cancers in 185 countries. CA: Cancer J 71(3):209–249. https://doi.org/10.3322/caac.21660
11. Kher C, Kumar S (2022) The application of nanotechnology and nanomaterials in cancer diagnosis and treatment: a review. Cureus 14(9):e29059. https://doi.org/10.7759/cureus.29059
12. Alshehri S, Imam SS, Rizwanullah M (2021) Progress of cancer nanotechnology as diagnostics, therapeutics, and theranostics nanomedicine: preclinical promise and translational challenges. Pharm 13:24. https://doi.org/10.3390/pharmaceutics13010024
13. Joudeh N, Linke D (2022) Nanoparticle classification, physicochemical properties, characterization, and applications: a comprehensive review for biologists. J Nanobiotechnol 20(1):262. https://doi.org/10.1186/s12951-022-01477-8
14. Shameli K, Ahmad MB, Yunus WM et al (2010) Green synthesis of silver/montmorillonite/chitosan bionanocomposites using the UV irradiation method and evaluation of antibacterial activity. Int J Nanomed 5:875–887. https://doi.org/10.2147/IJN.S13632
15. Tsuji M, Hashimoto M, Nishizawa Y (2005) Microwave-assisted synthesis of metallic nanostructures in solution. Chemistry (Weinheim an der Bergstrasse, Germany) 11(2):440–452. https://doi.org/10.1002/chem.200400417
16. Baig N, Kammakakam I, Falath W (2021) Nanomaterials: a review of synthesis methods, properties, recent progress, and challenges. Mater Adv 2:1821–1871. https://doi.org/10.1039/D0MA00807A
17. Kharissova OV, Kharisov BI, Oliva González CM (2019) Greener synthesis of chemical compounds and materials. R Soc Open Sci 6(11):191378. https://doi.org/10.1098/rsos.191378
18. Bahrulolum H, Nooraei S, Javanshir N et al (2021) Green synthesis of metal nanoparticles using microorganisms and their application in the agrifood sector. J Nanobiotechnol 19:86. https://doi.org/10.1186/s12951-021-00834-3

19. Hano C, Abbasi BH (2021) Plant-based green synthesis of nanoparticles: production, characterization and applications. Biomolecules 12(1):31. https://doi.org/10.3390/biom12010031
20. Chaudhary R, Nawaz K, Khan AK (2020) An overview of the algae-mediated biosynthesis of nanoparticles and their biomedical applications. Biomolecules 10(11):1498. https://doi.org/10.3390/biom10111498
21. Singh J, Dutta T, Kim KH et al (2018) 'Green' synthesis of metals and their oxide nanoparticles: applications for environmental remediation. J Nanobiotechnol 16:84. https://doi.org/10.1186/s12951-018-0408-4
22. Vidyasagar PRR, Singh SK et al (2023) Green synthesis of silver nanoparticles: methods, biological applications, delivery and toxicity. Mater Adv 4:1831–1849. https://doi.org/10.1039/D2MA01105K
23. Rahuman HBH, Dhandapani R, Narayanan S et al (2022) Medicinal plants mediated the green synthesis of silver nanoparticles and their biomedical applications. IET Nanobiotechnol 16(4):115–144. https://doi.org/10.1049/nbt2.12078
24. Pandit C, Roy A, Ghotekar S et al (2022) Biological agents for synthesis of nanoparticles and their applications. J King Saud Univ Sci 34(3):101869. https://doi.org/10.1016/j.jksus.2022.101869
25. Barabadi H, Noqani H, Ashouri F et al (2023) Nanobiotechnological approaches in anticoagulant therapy: the role of bioengineered silver and gold nanomaterials. Talanta 256:124279. https://doi.org/10.1016/j.talanta.2023.124279
26. Barabadi H, Mobaraki K, Ashouri F et al (2023) Nanobiotechnological approaches in antinociceptive therapy: animal-based evidence for analgesic nanotherapeutics of bioengineered silver and gold nanomaterials. Adv Colloid Interface Sci 316:102917. https://doi.org/10.1016/j.cis.2023.102917
27. Zhang Z, Liu Y, Lu M et al (2020) *Rhodiola rosea* extract inhibits the biofilm formation and the expression of virulence genes of cariogenic oral pathogen Streptococcus mutans. Arch Oral Biol 116:104762. https://doi.org/10.1016/j.archoralbio.2020.104762
28. Paladini F, Pollini M (2019) Antimicrobial silver nanoparticles for wound healing application: progress and future trends. Materials (Basel) 12(16):2540. https://doi.org/10.3390/ma12162540
29. Balan K, Qing W, Wang Y et al (2016) Antidiabetic activity of silver nanoparticles from green synthesis using *Lonicera japonica* leaf extract. RSC Adv 6:40162–40168. https://doi.org/10.1039/C5RA24391B
30. Ghosh R, Sarkhel S, Saha K et al (2021) Synthesis, characterization & evaluation of venom neutralization potential of silver nanoparticles mediated *Alstonia scholaris* Linn bark extract. Toxicol Rep 8:888–895. https://doi.org/10.1016/j.toxrep.2021
31. Khorrami S, Dogani M, Mahani SE et al (2023) Neuroprotective activity of green synthesized silver nanoparticles against methamphetamine-induced cell death in human neuroblastoma SH-SY5Y cells. Sci Rep 13(1):11867. https://doi.org/10.1038/s41598-023-37917-0
32. Wang L, Hu C, Shao L (2017) The antimicrobial activity of nanoparticles: present situation and prospects for the future. Int J Nanomed 12:1227–1249. https://doi.org/10.2147/IJN.S121956
33. Wahab S, Khan T, Adil M et al (2021) Mechanistic aspects of plant-based silver nanoparticles against multi-drug resistant bacteria. Heliyon 7(7):e07448. https://doi.org/10.1016/j.heliyon.2021.e07448
34. Singh P, Ali SW, Kale RD (2023) Antimicrobial nanomaterials as advanced coatings for self-sanitizing of textile clothing and personal protective equipment. ACS Omega 8(9):8159–8171. https://doi.org/10.1021/acsomega.2c06343
35. Subramanian P, Nishan M (2015) Biological activities of greater galangal, Alpinia galanga—a Review. Res Rev J Bot Sci:15–19
36. Imchen P, Ziekhru M, Zhimomi BK (2022) Biosynthesis of silver nanoparticles using the extract of Alpinia galanga rhizome and Rhus semialata fruit and their antibacterial activity. Inorg Chem Commun 142:109599. https://doi.org/10.1016/j.inoche.2022.109599
37. Wen C, Zhang J, Zhang H et al (2018) Advances in ultrasound assisted extraction of bioactive compounds from cash crops–a review. Ultrason Sonochem 48:538–549
38. Canovi M, Lucchetti J, Stravalaci M et al (2012) Applications of surface plasmon resonance (SPR) for the characterization of nanoparticles developed for biomedical purposes. Sensors (Basel, Switzerland) 12(12):16420–16432. https://doi.org/10.3390/s121216420
39. Cheng Z, Moore J, Yu L (2006) High-throughput relative DPPH radical scavenging capacity assay. J Agric Food Chem 54:7429–7436. https://doi.org/10.1021/jf0611668
40. Vichai V, Kirtikara K (2006) Sulforhodamine B colorimetric assay for cytotoxicity screening. Nat Protoc 1(3):1112–1116. https://doi.org/10.1038/nprot.2006.179
41. Krishnaraj C, Jagan EG, Rajasekar S et al (2010) Synthesis of silver nanoparticles using Acalypha indica leaf extracts and its antibacterial activity against water borne pathogens. Colloids Surf B 76(1):50–56. https://doi.org/10.1016/j.colsurfb.2009.10.008
42. Masum MMI, Siddiqa MM, Ali KA (2019) Biogenic synthesis of silver nanoparticles using *Phyllanthus emblica* fruit extract and its inhibitory action against the pathogen *Acidovorax oryzae* strain RS-2 of rice bacterial brown stripe. Front microbiol 10:820. https://doi.org/10.3389/fmicb.2019.00820
43. Dehghanizade S, Arasteh J, Mirzaie A et al (2018) Green synthesis of silver nanoparticles using Anthemis atropatana extract: characterization and in vitro biological activities. Artif Cells Nanomed Biotechnol 46(1):160–168. https://doi.org/10.1080/21691401.2017.1304402
44. Bilal M, Rasheed T, Iqbal HMN et al (2017) Development of silver nanoparticles loaded chitosan-alginate constructs with biomedical potentialities. Int J Biol Macromol 105(Pt 1):393–400. https://doi.org/10.1016/j.ijbiomac.2017.07.047
45. Zhang JZ, Noguez C (2008) Plasmonic optical properties and applications of metal nanostructures. Plasmonics 3:127–150. https://doi.org/10.1007/s11468-008-9066-y
46. Bilal M, Khan S, Ali J et al (2019) Biosynthesized silver supported catalysts for disinfection of Escherichia coli and organic pollutant from drinking water. J Mol Liq 281:295–306. https://doi.org/10.1016/j.molliq.2019.02.087
47. Qais FA, Shafiq A, Khan HM et al (2019) Antibacterial effect of silver nanoparticles synthesized using Murraya koenigii (L.) against multidrug-resistant pathogens. Bioinorg Chem and Appl. https://doi.org/10.1155/2019/4649506
48. Ahmed S, Ahmad M, Swami BL et al (2016) A review on plants extract mediated synthesis of silver nanoparticles for antimicrobial applications: a green expertise. J Adv Res 7(1):17–28. https://doi.org/10.1016/j.jare.2015.02.007
49. Raghunandan D, Bedre MD, Basavaraja S et al (2010) Rapid biosynthesis of irregular shaped gold nanoparticles from macerated aqueous extracellular dried clove buds (Syzygium aromaticum) solution. Colloids Surf B 79(1):235–240. https://doi.org/10.1016/j.colsurfb.2010.04.003
50. Praba PS, Vasantha VS, Jeyasundari J et al (2015) Synthesis of plant-mediated silver nanoparticles using Ficus microcarpa leaf extract and evaluation of their antibacterial activities. Eur Chem Bull 4(3):116–120. https://doi.org/10.17628/ECB.2015.4.117-120
51. Vanlalveni C, Lallianrawna S, Biswas A et al (2021) Green synthesis of silver nanoparticles using plant extracts and their antimicrobial activities: a review of recent literature. RSC Adv 11(5):2804–2837. https://doi.org/10.1039/d0ra09941d

52. Mariadoss AVA, Ramachandran V, Shalini V et al (2019) Green synthesis, characterization and antibacterial activity of silver nanoparticles by Malus domestica and its cytotoxic effect on (MCF-7) cell line. Microb Pathog 135:103609. https://doi.org/10.1016/j.micpath.2019.103609
53. Ahn EY, Jin H, Park Y et al (2019) Assessing the antioxidant, cytotoxic, apoptotic and wound healing properties of silver nanoparticles green-synthesized by plant extracts. Mater Sci Eng C 101:204–216. https://doi.org/10.1016/j.msec.2019.03.095
54. Rani P, Kumar V, Singh PP et al (2020) Highly stable AgNPs prepared via a novel green approach for catalytic and photocatalytic removal of biological and non-biological pollutants. Environ Int 143:105924. https://doi.org/10.1016/j.envint.2020.105924
55. Kanniah P, Balakrishnan S, Subramanian ER (2023) Preliminary investigation on the impact of engineered PVP-capped and uncapped silver nanoparticles on Eudrilus eugeniae, a terrestrial ecosystem model. Environ Sci Pollut Res Int 30(10):25239–25255. https://doi.org/10.1007/s11356-022-21898-0
56. Soshnikova V, Kim YJ, Singh P et al (2018) Cardamom fruits as a green resource for facile synthesis of gold and silver nanoparticles and their biological applications. Artif Cells Nanomed Biotechnol 46(1):108–117. https://doi.org/10.1080/21691401.2017.1296849
57. Chen L, Huo Y, Han YX et al (2020) Biosynthesis of gold and silver nanoparticles from Scutellaria baicalensis roots and in vitro applications. Appl Phy A 126:1–12. https://doi.org/10.1007/s00339-020-03603-5
58. Yap YH, Azmi AA, Mohd NK et al (2020) Green synthesis of silver nanoparticle using water extract of onion peel and application in the acetylation reaction. Arab J Sci Eng 45:4797–4807. https://doi.org/10.1007/s13369-020-04595-3
59. Elumalai D, Hemavathi M, Deepaa CV et al (2017) Evaluation of phytosynthesised silver nanoparticles from leaf extracts of *Leucas aspera* and *Hyptis suaveolens* and their larvicidal activity against malaria, dengue and filariasis vectors. Parasite Epidemiol Control 2(4):15–26. https://doi.org/10.1016/j.parepi.2017.09.001
60. Shanmuganathan R, Ali DM, Prabakar D et al (2018) (2018) An enhancement of antimicrobial efficacy of biogenic and ceftriaxone-conjugated silver nanoparticles: green approach. Environ Sci Pollut Res 25(11):10362–10370. https://doi.org/10.1007/s11356-017-9367-9
61. Chandrakala V, Aruna V, Angajala G (2022) Review on metal nanoparticles as nanocarriers: current challenges and perspectives in drug delivery systems. Emergent Mater 5(6):1593–1615. https://doi.org/10.1007/s42247-021-00335-x
62. Balmain A, Gray J, Ponder B (2003) The genetics and genomics of cancer. Nat Genet 33(Suppl):238–244. https://doi.org/10.1038/ng1107
63. Reddy NJ, Nagoor VD, Rani M et al (2014) Evaluation of antioxidant, antibacterial and cytotoxic effects of green synthesized silver nanoparticles by Piper longum fruit. Mater Sci Eng C 34:115–122. https://doi.org/10.1016/j.msec.2013.08.039
64. Heydari R, Rashidipour M (2015) Green synthesis of silver nanoparticles using extract of oak fruit hull (jaft): synthesis and in vitro cytotoxic effect on mcf-7 cells. Int J Breast Cancer 2015:846743. https://doi.org/10.1155/2015/846743
65. Venugopal K, Rather HA, Rajagopal K et al (2017) Synthesis of silver nanoparticles (AgNPs) for anticancer activities (MCF 7 breast and A549 lung cell lines) of the crude extract of Syzygium aromaticum. J Photochem Photobiol B Biol 167:282–289. https://doi.org/10.1016/j.jphotobiol.2016.12.013
66. Dey S, Fageria L, Sharma A et al (2022) Silver nanoparticle-induced alteration of mitochondrial and ER homeostasis affects human breast cancer cell fate. Toxicol Rep 9:1977–1984. https://doi.org/10.1016/j.toxrep.2022.10.017
67. Manke A, Wang L, Rojanasakul Y (2013) Mechanisms of nanoparticle-induced oxidative stress and toxicity. BioMed Res Int 2013:942916. https://doi.org/10.1155/2013/942916
68. Rinna A, Magdolenova Z, Hudecova A et al (2015) Effect of silver nanoparticles on mitogen-activated protein kinases activation: role of reactive oxygen species and implication in DNA damage. Mutagenesis 30:59–66. https://doi.org/10.1093/mutage/geu057
69. Mebratu Y, Tesfaigzi Y (2009) How ERK1/2 activation controls cell proliferation and cell death: is subcellular localization the answer? Cell Cycle 8:1168–1175. https://doi.org/10.4161/cc.8.8.8147
70. Eom HJ, Choi J (2010) p38 MAPK activation, DNA damage, cell cycle arrest and apoptosis as mechanisms of toxicity of silver nanoparticles in Jurkat T cells. Environ Sci Technol 44:8337–8342. https://doi.org/10.1021/es1020668
71. Hudecová A, Kusznierewicz B, Rundén-Pran E et al (2012) Silver nanoparticles induce premutagenic DNA oxidation that can be prevented by phytochemicals from Gentiana asclepiadea. Mutagenesis 27:759–769. https://doi.org/10.1093/mutage/ges046
72. Dakal TC, Kumar A, Majumdar RS et al (2016) Mechanistic basis of antimicrobial actions of silver nanoparticles. Front Microbiol 7:1831. https://doi.org/10.3389/fmicb.2016.01831
73. Liu X, Shan K, Shao X et al (2021) Nanotoxic effects of silver nanoparticles on normal HEK-293 cells in comparison to cancerous HeLa cell line. Int J Nanomedicine 16:753–761. https://doi.org/10.2147/IJN.S289008
74. Chou CC, Riviere JE, Monteiro-Riviere NA (2003) The cytotoxicity of jet fuel aromatic hydrocarbons and dose-related interleukin-8 release from human epidermal keratinocytes. Arch Toxicol 77(7):384–391
75. Sukirtha R, Priyanka KM, Antony JJ et al (2012) Cytotoxic effect of Green synthesized silver nanoparticles using Melia azedarach against in vitro HeLa cell lines and lymphoma mice model. Process Biochem 47(2):273–279. https://doi.org/10.1016/j.procbio.2011.11.003
76. Sriranjani R, Srinithya B, Vellingiri V et al (2016) Silver nanoparticle synthesis using Clerodendrum phlomidis leaf extract and preliminary investigation of its antioxidant and anticancer activities. J Mol Liq 220:926–930. https://doi.org/10.1016/j.molliq.2016.05.042
77. Botcha S, Prattipati SD (2020) Callus extract mediated green synthesis of silver nanoparticles, their characterization and cytotoxicity evaluation against MDA-MB-231 and PC-3 cells. Bionanoscience 10:11–22. https://doi.org/10.1007/s12668-019-00683-3